Towards a structural understanding of plant-microbiota interactions using cryo-EM techniques

Liedtke, J.

6

Distribution of temperate bacteriophages among endophytic Bacteroidota and their relevance

Members of the phylum Bacteroidota play a key role in diverse microbiota and influence the health and resilience of their hosts and their associated microbial communities. Due to their often-unique metabolic capabilities and mutualistic behaviour, they are being investigated as alternative treatments to improve plant resistance in agriculture and soil remediation. Recent studies suggest that some of these beneficial traits may be linked to the presence of phage-derived genetic elements within the bacterial genome. Understanding how prophages influence their behaviour, competitiveness and interactions within the plant-associated microbiota is essential for their effective and sustainable application.

In this study, we explored the distribution and inducibility of prophages in selected endophytic members of the phylum Bacteroidota. The resulting extracts were tested for lytic activity, and their host spectrum was assessed. In several cases, phage-like particles were visualised using transmission electron microscopy. The observed lytic activity and visualisation of phage-like particles indicate the presence of inducible prophages in endophytic Bacteroidota. These findings support the need for further investigation into prophage activity in endophytic Bacteroidota and may contribute to a better understanding of their role in the plant-associated microbiota.

This chapter is based on **Liedtke, J.**, Martina, I.N., Posthuma, K., and Briegel, A.: Distribution of temperate bacteriophages among endophytic Bacteroidota and their relevance, in preparation.

6.1 Introduction

The phylum Bacteroidota is one of the dominant phyla in various microbial communities, known as microbiota, including soil and plant microbiota [8]. This dominance is largely due to their ability to degrade complex organic compounds. With a few exceptions, they exhibit predominantly mutualistic behaviour, contributing to both the health of their host (plant) and the surrounding microbiota [8]. In addition, previous studies have shown that the endophytic members *Flavobacterium anhuiense* and *Chitinophaga pinensis*, which can colonize and reside in plant tissue, significantly improve the plant's resilience [85]. These properties make them promising candidates for the development of sustainable and environmentally friendly treatments in agriculture as alternatives to pesticides and antibiotics.

In addition to their beneficial traits, these bacteria display intriguing adaptive responses under certain conditions that remain poorly understood. One such response is the pronounced morphological plasticity observed in *C. pinensis* (Chapter 3) and *F. anhuiense* (unpublished). In both cases, cells transition from several micrometer long filamentous cells to markedly smaller morphotypes of less than 1 µm. The underlying triggers of these repeated transitions remain to be elucidated (Chapter 3). These phenotypic changes may influence bacterial interactions within the microbiota. To fully harness their potential for sustainable agricultural applications, it is crucial to understand how these bacteria interact with the plant microbiota in response to such changes.

Microbiota are multi-species associations where interactions occur at different levels (species, population, individuals) with competitive, supportive, facilitative, or suppressive dynamics. These interactions can change over time or in response to environmental conditions. Microbiota also include viruses that target bacteria, known as phages (bacteriophages), which play a key role in microbiota diversity. According to the 'kill the winner'theory [9], phages target bacteria that thrive under certain conditions. As a consequence they prevent the overgrowth of a single species, thereby shaping the microbiota composition, maintaining its diversity, and ensuring its long-term persistence. Although phages can exert strong selective pressure on bacterial populations, bacteria have developed adaptive strategies to evade infection. Among these, morphological changes that reduce or eliminate phage-binding proteins on the cell surface have been proposed as a potential escape mechanism [168, 169].

This theory applies to phages in the lytic replication cycle, which hijack the host's replication system to predominantly produce phage particles, released after assembly through cell lysis. In contrast, some phages integrate their genome into that of their host, entering the lysogenic replication cycle. Their sequence remains dormant as a prophage and is replicated together with the host until a trigger induces the switch to the lytic cycle. Prophages are not necessarily disadvantageous to the host. Under certain conditions they can benefit the host by conferring additional metabolic capabilities [10, 170], resistance traits [11] or morphological changes [12] that provide a competitive advantage within the community. Nonetheless, prophage induction has also been associated with host stress responses. For instance, host cell filamentation has been identified as part of an SOS response triggered by prophage induction [171]. Notably, filamentous cells are more susceptible to phage infection compared to smaller cell sizes [12].

Prophages are widespread among bacterial genomes and may contribute to enhanced microbiota resilience and the stabilisation of microbial community dynamics under stressful environmental conditions. Whether such elements are also present in endophytic Bacteroidota and potentially contribute to traits relevant for their lifestyle has not been systematically investigated.

In this study, we explored prophage distribution in endophytic members of the Bacteroidota, including representatives of the classes: Chitinophagia, Sphingobacteriia, Cytophagia and Flavobacteriia. We also examined whether the observed morphological changes in *C. pinensis* and *F. anhuiense* may be linked to the presence or inducibility of prophages.

6.2 Material & Methods

6.2.1 Bacterial strains and culture conditions

The following bacterial strains of the phylum Bacteroidota were used for prophage induction and isolation, selected on the basis of prophage prediction: *Flavobacterium anhuiense* (98) [85], *Chitinophaga pinensis* (94) wild-type [85], *Chitinophaga pinensis* lab-strain (DSM 2588), and *Runella defluvii* (DSM 17976). These strains were grown in 0.1x TSB at 25 °C. The following strains *Chitinophaga jiangningensis* (DSM 27406), *Chitinophaga niabensis* (DSM 24787), *Dyadobacter endophyticus* (DSM 100786), *Flavobacterium johnsoniae subsp. johnsoniae* (DSM 2064), *Mucilaginibacter auburnensis* (DSM 28175), *Niabella soli* (DSM 19437), and *Solitalea koreensis* (DSM 21342) were grown in LB at 28 °C. Strains were cultured overnight in liquid media at their respective temperatures and 200 rpm. Additionally, a *Flavobacterium* sp. strain, obtained from a collaborator's strain collection (B. Ford; Utrecht University), was included. The strain was not further characterized but is known to belong to the genus *Flavobacterium*. Although its genome sequence was unavailable for prophage prediction, it was included in the induction assays and lytic activity screening to assess potential susceptibility. This strain was cultured in 0.1x TSB at 25 °C, under the same conditions as for *F. anhuiense*.

6.2.2 Prediction of prophage elements

The web-based tools Prophage-Hunter [172] and PHASTER [173–175] were used to identify prophage regions and assess their predicted completeness (classified as active, ambiguous, or inactive). Genome sequences were obtained from NCBI GenBank, except for *Chitinophaga pinensis* (94) and *Flavobacterium anhuiense* (98), which were obtained from Carrión (2019) [85].

6.2.3 Prohage induction assays

Induction with mitomycin C

Prophage induction using mitomycin C (final concentrations: 1.5 and 2.5 mM) was performed in overnight cultures incubated at strain specific temperature and 250 rpm. Optical density at 600 nm (OD_{600}) was monitored, and samples were collected every 2 h during the first 6 h, and at 24 h and 48 h. All samples were filtered through 0.22 µm filters and stored at 4 °C.

Induction with UV-light

Overnight cultures (5 ml) were transferred to sterile petri dishes (Ø 9 cm) and placed without a lid at a distance of 15 cm from the UV-light source (6W Germicidal light T5 Tube UVC sterilizer, Lcamaw via Aliexpress.nl). Samples were collected after 1, 4, 10, and 20 min of exposure and briefly cooled on ice. Each sample was divided equally. One part was filtered (0.22 µm) and stored as described above. The other part was added to inoculate an equal volume of media and incubated under strain specific conditions to obtain potentially phage-free strains.

Unless stated otherwise, all filtered samples obtained from these assays are hereafter referred to as extracts.

6.2.4 Screening for lytic phage activity

All extracts obtained from induction assays were screened for lytic activity using plaque assay techniques, which were also used for isolation and purification.

Preparation of double-overlay plates

For double-overlay plates (21 cm x 21 cm), the basal agar layers were prepared with 1.5% (w/v) agar using strain-specific growth medium. The strain suspensions for the top agar layer were obtained from overnight cultures, centrifuged (3,000x g; 5 min) and the cell pellet resuspended in phage buffer to an OD_{600} of 0.1. Subsequently, 1 ml of each strain suspension was combined with 11 ml of liquefied medium containing 0.5% (w/v) low-melting-point agar, stored at 45 °C. Shortly before pouring over the basal agar layer, 12 µl of 5 M $CaCl_2$ was added. Once the top agar was solidified, the plates were ready for the plaque assays.

Lytic activity screening and host range determination

Extract from induction assays were screened for lytic activity using spot assays in which 3 µl extract was spotted in triplicates onto double-overlay plates. This approach avoids dilution of the potential phage concentration and increases the probability of observing plaques. After diffusion, the plates were incubated at the respective optimal temperature for each strain and observed daily for two weeks.

Plates displaying visible plaques were subsequently used for phage isolation and purification. Individual plaques were sampled using sterile toothpicks or sterile cotton swabs, which were moistened with phage buffer prior use. These were streaked onto double-overlay plates prepared with the respective host strain. The plates were incubated and observed daily for up to two weeks, with smaller plaques used for further rounds of purification. Furthermore, a dilution series (10^0 to 10^{-5}) of the extracts showing lytic activity was prepared in phage buffer, and each dilution step was tested in triplicate, resulting in countable small plaques [176].

In addition, extracts and concentrates were tested for lytic activity against the aforementioned strains using the double-overlay assay. This method was used to determine the host range of the extracts, based on the formation of plaques and changes in colony morphology.

Concentrate potential phage particles and size segregation

To concentrate potential phage particles and facilitate imaging by TEM, the extracts were subjected to filtration using different pore sizes and precipitation. For filtration, 400 µl of the extract was transferred to microcentrifuge filters (AmiconUltra; - 100 K; 100,000 NMWL; Ultracel ®; Merck Milipore Ltd; Cork; IE) and centrifuged (1,500x g; 30 min). The remaining volume in the filter, assumed to contain concentrated phage particles, was transferred to a new tube (1.5 ml) and stored at 4 °C. The filtrates were further treated with smaller pore size filters (AmiconUltra; Ultra -15; Ultracel ® - 10K; 10,000 NMWL; Merck Milipore Ltd; Cork; IE) and centrifuged (5,000x g; 10 min; 4 °C), resulting in further concentration of potential smaller phages and removal of cell debris. The final concentrates were tested for lytic activity as previously described. The plaque forming concentrates were used for phage isolation, purification and TEM analysis. As a concentration method, PEG-based precipitation was applied using a modified protocol from Ambros *et al.* (2023). In this procedure, 900 µl of extract was supplemented with 300 µl of 20% (w/v) PEG8,000 (final concentration: 4%; Sigma-Aldrich) and 300 µl of 2.5 M NaCl (final concentration: ~3%), followed by incubation on ice for at least 1 h. Subsequently, the samples were centrifuged (13,000x g; 10 min; 4 °C) and the resulting pellet was resuspended in phage buffer at 10% of the originally used sample volume. Tests were repeated without NaCl and with PEG6,000 (Sigma-Aldrich) to account for potential sensitivity of phage particles to high salt concentration or PEG type. Concentrates were screened for lytic phage activity, with plaque-forming samples subjected to further isolation, purification, and TEM imaging.

6.2.5 Transmission electron microscopy

All extracts and concentrates were screened for the presence of phage particles and imaged using TEM (Talos L120c; 120 kV; Thermo Ficher Scientific). For this purpose, 3 µl of each sample were incubated for 30 sec. on a glow-discharged carbon coated grid (CF200-CU-50; Electron microscopy science). Excess liquid was removed and the remaining sample on the grid negatively stained with 4% (w/v) uranyl acetate for 30 sec. Initially, imaging was performed without gold beads. However, to facilitate focusing and ease imaging, a 1/25 dilution of 10-nm colloidal gold solution treated with protein A (Cell Microscopy Core, Utrecht University, Utrecht, The Netherlands) was added to the sample prior to negative staining.

6.3 Results

6.3.1 Detection of active prophages regions among Bacteroidota strains

To investigate the presence of prophages within the phylum Bacteroidota, a selection of strains relevant to plant-associated habitats, were analysed. Genomic sequences of these strains were retrieved from the NCBI database and screened for the presence of prophage sequences within the bacterial genome using the web-based tools Prophage-hunter and PHASTER. The results were categorized based on sequence completeness scores, with classifications into active, ambiguous, and inactive prophages. The outcome of the prophage prediction is summarized in table 6.1.

Table 6.1: Summary of prophage predictions for 13 Bacteroidota strains, using the Prophage-hunter tool [172]. Genomic data were retrieved from the NCBI database and screened for the presence of prophage regions, which were categorized as active, ambiguous or inactive based on completeness scores. Sequences of the wild-type strains *Chitinophaga pinensis* (94) and *Flavobacterium anhuiense* (98) were obtained from Carrión (2019) [85].

Class	Name	Strain no.	Predicted	Inactive	Ambiguous	Active
Chitinophagia	*C. niabensis*	DSM24787	126	120	3	3
	C. pinensis	DSM2588	131	128	4	3
	C. jiangningensis	DSM27406	171	162	6	3
	N. soli	DSM19437	79	70	8	1
	C. pinensis (94)*	—	110	99	7	4
Sphingobacteriia	*S. koreensis*	DSM21342	111	108	2	1
	M. auburnensis	DSM28175	79	78	1	0
Cytophagia	*R. defluvii*	DSM17976	238	217	9	10
	D. endophyticus	DSM100786	170	155	12	3
Flavobacteriia	*F. johnsoniae*	DSM2064	178	148	25	5
	F. anhuiense (98)*	—	101	87	12	2
Bacteroidia	*A. hydrogenigenes*	DSM24657	115	110	3	2

* wild-type strains; internal identifiers (94) and (98) as used by Carrión et al. [85]

While PHASTER detected a single, previously described prophage (FpV-21) in *Flavobacterium johnsoniae* [177], Prophage-hunter idetified identified substantially more prophage sequences across a broader range of strains (Tab. 6.1). Among the selected strains, *Runella defluvii* had the highest number of predicted prophages sequences, with a total of 238, of which 10 were classified as active (Tab. 6.1). Whereas in *Mucilaginibacter auburnensis*, a total of 79 sequences were found, of which only one was ambiguous and none were classified as active (Tab. 6.1). Despite these predictions, *M. auburnensis* was nevertheless included in the further investigation, as a potentially susceptible strain that could support phage proliferation and enrichment.

Following induction, all 12 selected strains produced extracts with detectable lytic activity. Differences were observed in the timing at which these extracts led to plaque formation. In some cases, lytic activity was detectable as early as 2 h post-induction, while in others, plaque formation appeared 6 h after induction. In all cases, lytic activity was detectable within 24 h post-induction. In addition, induction with UV-light resulted in larger plaques compared to the mitomycin C induced samples.

To quantify the potential phage concentration in the extracts with lytic activity, a dilution series was performed. With each dilution step, lytic activity gradually decreased with plaque signals fading below the threshold of reliable detection (Fig. 6.1B). Therefore, extracts were subsequently concentrated, which led to more distinct plaque formation. Nevertheless, the concentration of lytic particles remained below the quantification limit under standard assay conditions. During the experiment, we also observed the formation of "white plaques" (Fig. 6.1C). These were not considered to be indicators of lytic infection, as they lacked complete cell lysis and distinct plaque formation. In four of the 12 extracts, plaque formation was observed on the respective strain of origin. *Chitinophaga pinensis* (DSM 2588), *M. auburnensis*, *R. defluvii*, and *Flavobacterium anhuiense* indicating that these strains were susceptible to reinfection.

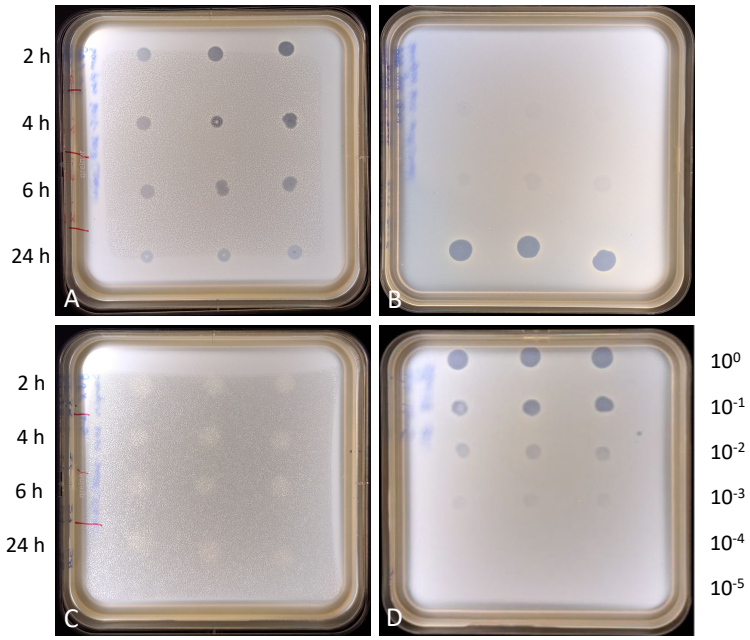

Figure 6.1: Plaque assays: Plaque formation after 2, 4, 6 and 24 h (A–C) with the appearance of bull's eye colonies (A), an increase of lytic activity over time after induction with mitomycin C (B), and the appearance of "white plaques" (C). The latter were considered as negative for plaque formation, as they did not lead to full cell lysis and formation of clear plaques. A dilution series (10^0 to 10^{-5}) of extract was performed to determine potential phage concentration. However, plaques gradually faded without forming smaller, countable plaques (D). (A) *Flavobacterium anhuiense* (98) infected with P10 derived from *Flavobacterium johnsoniae*. (B + D) *Chitinophaga pinensis* (94) infected with P3 derived from *Chitinophaga jiangningensis*. (C) *F. anhuiense* (98) infected with P12 derived from *Flavobacterium* sp.

6.3.2 Host range of extracts with lytic activity

In the following, the extracts derived from the 12 different host strains are referred to as "the 12 extracts (P1–P12)" for better understanding (Tab. 6.2). The host-range assay revealed that all extracts (P1–P12) led to plaque formation when tested with susceptible strains (Tab. 6.2). The most susceptible strain was the lab strain *C. pinensis* (DSM 2588), which was susceptible to 11 extracts, followed by *M. auburnensis*, with susceptibility to 9, and *R. defluvii*, with susceptibility to 8 of the 12 extracts (Tab. 6.2). Of the 12 tested strains, 5 were susceptible to only one extract, which was derived either from *Chitinophaga niabensis* (P1) or *C. jiangningensis* (P3). The extract (P12) from *Flavobacterium* sp. showed lytic activity exclusively against *F. johnsoniae*. The remaining extracts (P1–P11) displayed lytic activity against 3 to 5 different strains.

6.3.3 TEM-based identification of phage-like structures

To confirm the presence of phages in the extracts and to determine their morphology, all extracts were analysed by negative staining and TEM. In three out of 12 extracts, assembled phages and phage like components such as capsids, tail fibres, and sheaths were observed. Phage-particle concentration appeared low, across the analysed samples,

Table 6.2: Host range of extracts. Summary of lytic activity screening performed against the strains used in the prophage induction assays. The extracts (P1–P12) were obtained from the strains listed in the left column by prophage induction assays, where P1 correspond to the first strain (*Chitinophaga niabensis*), P2 to the second (*Chitinophaga pinensis*), and so on. Each extract was first tested against its strain of origin and then against all other strains to determine host specificity.

Class	Strain	P1	P2	P3	P4	P5	P6	P7	P8	P9	P10	P11	P12
Chitinophagia	*C. niabensis*	–	–	+	–	–	–	–	–	–	–	–	–
	C. pinensis	+	+	+	+	+	+	+	+	+	+	+	–
	C. jiangningensis	+	–	–	–	–	–	–	+	+	–	–	–
	N. soli	–	–	+	–	–	–	–	–	–	–	–	–
	*C. pinensis**	–	–	+	–	–	–	–	–	–	–	–	–
Sphingobacteriia	*S. koreensis*	–	–	+	–	–	–	–	–	–	–	–	–
	M. auburnensis	+	+	–	+	+	+	+	+	+	–	+	–
Cytophagia	*R. defluvii*	+	+	–	+	+	–	+	+	+	+	–	–
	D. endophyticus	+	–	–	–	–	–	–	–	–	–	–	–
Flavobacteriia	*F. johnsoniae*	–	–	–	–	–	+	–	–	–	–	+	+
	*F. anhuiense**	–	–	–	–	+	+	–	+	–	+	+	–
	Flavobacterium sp.	–	–	–	–	+	+	–	–	–	–	–	–

* Wild-type strains [85]

including concentrates with only a few fully assembled phages detectable by TEM (Fig. 6.2). In some cases, structures resembling partial phage components were observed but could not be unambiguously identified. For example, extract (P12) of *F. johnsoniae* contained particles resembling capsids, along with numerous thin, needle like structures. Some of these structures appeared to be connected to capsid-like particles and were interpreted as potential phage tails (Fig. 6.2C). The capsid-like particles in this extract (P12) measured approx. 65–75 nm in diameter, while the associated tail-like structure ranged from 85–105 nm in length. Based on these dimensions and overall appearance, the morphology was tentatively assigned to the siphovirus morphotype. The tail-like structure appeared non-contractile under the observed conditions, but further analysis would be required to confirm its structural properties.

In contrast, extract P7 *M. auburnensis* revealed two morphologically distinct siphovirus-like phages. These two phages differed primarily in capsid sizes: one had a capsid with a diameter of approx. 65 nm(Fig. 6.2A), the other with a diameter of approx. 34 nm (Fig. 6.2B). The tail of the larger phage appeared flexible and measured 170–180 nm (Fig. 6.2A), whereas the smaller phage had a shorter and visually more rigid tail of approx. 160–165 nm (Fig. 6.2B). Neither phage displayed retracted sheaths. Occasionally, tangled tail tips were observed in the larger phage (Fig. 6.2A), while the smaller phage appeared to lack a defined tail tip (Fig. 6.2B). Notably, the smaller phage was considerably less abundant, with only a few observed particles observed.

Extract P3 *C. jiangningensis* contained numerous phage-like structures, predominantly sheath-like structures, many of which were loosely arranged (Fig. 6.2D-F). A few complete myovirus-like phages were identified showing typical morphology with capsids, inner tail tubes, sheaths, and base-plates (Fig. 6.2D-F). The capsid diameter was approx. 80–90 nm, and tail length ranged from 105–135 nm. T he remaining extracts did not show intact phage particles under the conditions used.

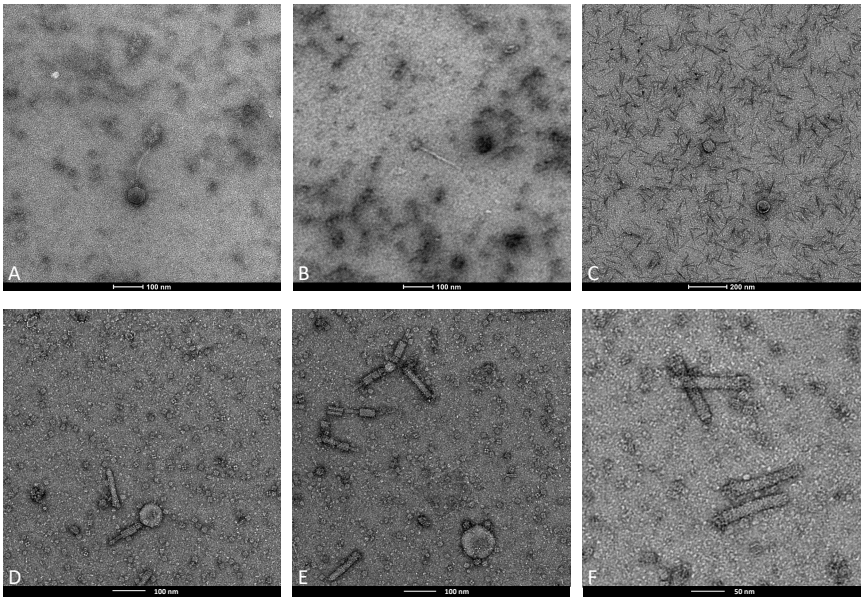

Figure 6.2: TEM images of phage particles in extracts. (A-B) Phages particles observed in P7 derived from *M. auburnensis*, displaying two morphologically distinct phage particles consistent with siphovirus morphology, (A) one with a capsid size of approx. 65 nm and (B) one with a capsid size of approx. 34 nm. (C) Phage-like particle from extract P12 (*F. johnsoniae*) showing morphology consistent with siphovirus. Capsid diameter measured approx. 65–75 nm. The extract P12 also contained numerous needle-like structures (85–105 nm in length), which were considered potential tail fibres. (D-F) Phage-like particles observed in extract P3 (*C. jiangningensis*), showing myovirus morphology. Predominant structures include partially and fully assembled sheath-like particles. (F) At higher magnification assembled base-plates can be observed on assembled sheaths. The capsid size of the P3 phage is about 80–90 nm in diameter, and the tail length ranged from 105–135 nm.

6.4 Discussion

Phages are known to significantly influence the diversity and composition of the microbial communities. They affect their hosts in various ways, including metabolic modulation and morphological alteration. Through these host-directed effects, phages may indirectly shape interspecies interactions within the microbiota, including its relationship with the superhost (plant). This raises the question of how much the observed morphological changes in *C. pinensis* (chapter 3) can be attributed to the presence or activity of phages.

To explore the distribution of prophages within the phylum Bacteroidota, especially in endophytic strains, computational prediction tools were used. These tools enable the identification of phage regions within bacterial genomes, regardless of whether they are transcriptionally active or dormant [178]. The analysis revealed prophage regions in all investigated Bacteroidota classes, with most strains carrying multiple sequences.

Their inducibility and lytic activity were then investigated, both towards the strain of origin and across the set of tested strains. As a result, all extracts exhibited lytic activity with a broad host range. Interestingly, phage activity was observed in the induced prophage extract from *M. auburnensis* (P7), despite the absence of a predicted active prophage in its genome based on current tools (Tab. 6.1). The presence of phage-particles in *M. auburnensis*

extract (P7) was confirmed by TEM analysis and two distinct phage morphologies were observed (Figure 6.2). The acquired images revealed two distinct phage morphologies.

In recent years, various computational tools and pipelines have been developed to predict and identify prophage regions within bacterial genomes. These tools are now widely accessible to a broader scientific community. However, they rely on databases and statistical methods that are often based on homology. As a result, these tools tend to detect only known or closely related prophage sequences, leaving divergent or novel sequences unrecognized. Recent improvements, such as the use of genomic features like dinucleotide relative abundance, aim to reduce false negatives. Nevertheless, no single tool currently available can capture the full diversity of prophages [179], and despite recent advancements, inaccuracies still occur. This underlines the importance of culture-based validation methods.

The inducibility of prophages can vary depending on factors like growth medium, temperature, and the type of induction applied. Standard triggers such as UV light and mitomycin C, do not induce all prophages, as their specific induction requirements are unknown. Furthermore, the presence of multiple prophages within the same host genome, also known as polylysogeny, may influence inducibility [180, 181].

In addition to active prophage sequences, inactive and cryptic phage sequences may also respond to induction. Their response could involve enzymatic activity with potential bactericidal effects. Such effects might explain the appearance of "white plaques" observed during the host range plaque assays (Fig. 6.1). Similar phenomena have been described for phage-derived structure as tailocins, which can be used by host bacteria to suppress competitors [182].

The presence of diverse prophage elements across strains suggests that such traits may support community resilience, particularly under fluctuating conditions [183]. However, prophage and phage sequence elements within the host genome come with certain costs and impact the host fitness by increasing energy demand and slowing host growth. Thus, the benefits must outweigh the costs, enabling the host to survive within the competition of the microbiota. The regulatory effect of the 'kill-the-winner'principle could potentially outweigh the negative fitness impact and support the persistence of slower growing strains.

This idea may be reflected in our observations comparing *C. pinensis* (94) and *F. anhuiense* (98), both of which originated from the same endophytic microbiota. While *C. pinensis* exhibited slower growth, it showed the lowest susceptibility in the plaque assays. Conversely, *F. anhuiense* was susceptible to the extract derived from *C. pinensis* (94), but not vice versa.

Compared to the wild type strain (94), the lab strain *C. pinensis* (DSM 2588), which exhibited similar growth rates showed the highest susceptibility in the assays and was also susceptible to extracts from *F. anhuiense*. While the lab strain carried a higher total number of predicted prophage regions (131 vs. 110), the wild-type strain had more regions classified ambiguous or active. These differences may reflect functional variation in prophage content and could help explain both the variation in susceptibility and the slightly earlier onset of morphological transition observed in the wild-type strain. In addition, no plaque formation was observed in 75% of the strains when exposed to their own extract (Tab. 6.2), suggesting possible resistance mechanisms, potentially mediated by resident prophages.

This observation is consistent with previous studies suggesting that phage-associated factors can influence host cell morphology and modulate susceptibility [168, 169].

Through polylysogeny, multiple prophage-encoded resistance mechanisms can accumulate within the host genome. These coexisting prophage regions may modulate each other's inducibility. However, the hierarchical order of their inducibility and their regulatory effects on one another are not yet well understood.

In addition to their intro-host effects, phage elements, both free and integrated, can indirectly influence the superhost (plant) by modulating bacterial metabolism. These changes may alter the turnover of secondary metabolites and availability of nutrients and trace elements. Under stress conditions, phages may serve as a regulatory mechanisms that limits the overgrowth of individual strains. This in turn, may protect the superhost from both potential exploitation and destabilization of its microbiota.

Overall, this study provides first insights into the distribution and inducibility of prophages, as well as the potential host spectrum of their inducible lytic counterparts in endophytic Bacteroidota. These findings lay the groundwork for future investigations into the ecological roles and functional impacts of phages in plant-associated microbiota. In particular, the characterization of inducible prophages and cryptic phage elements may help clarify their contribution to the endophytic lifestyle and to the morphological plasticity observed in certain strains. Furthermore, exploring whether plant-derived compounds, such as root exudates, can trigger prophage induction would deepen our understanding of the regulatory dynamics between the plant as superhost and its microbiota.

Acknowledgements

TEM images were collected at the Netherlands Centre for Electron Nanoscopy (NeCEN) at Leiden University. This work benefited from access to NeCEN, which was funded in part by the Netherlands Electron Microscopy Infrastructure (NEMI), project number 184.034.014 of the National Roadmap for Large-Scale Research Infrastructure of the Dutch Research Council (NWO). J.L. was supported by the OCENW.GROOT.2019.063 and Building Blocks of Life 737.016.00 grants from the Netherlands Organization for Scientific Research (NWO), both awarded to A.B.

Author Contribution

J.L. conceived and designed the study, supervised the project, advised both students, and wrote the manuscript. I.N.M. and K.P. conducted the experimental work as part of their respective Bachelor theses, under the supervision of J.L. A.B. supervised the overall study and provided conceptual guidance and feedback on the manuscript.